

Chemistry in Motion: Tiny Synthetic Motors

Peter H. Colberg, Shang Yik Reigh, Bryan Robertson, and Raymond Kapral*

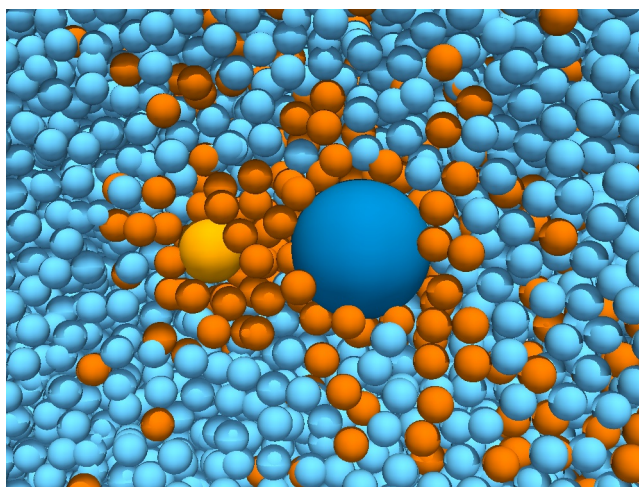
*Chemical Physics Theory Group, Department of Chemistry,
University of Toronto, Toronto, Ontario M5S 3H6 Canada*

E-mail: rkapral@chem.utoronto.ca

Conspectus

Diffusion is the principal transport mechanism that controls the motion of solute molecules and other species in solution; however, the random walk process that underlies diffusion is slow and often non-specific. Although diffusion is an essential mechanism for transport in the biological realm, biological systems have devised more efficient transport mechanisms using molecular motors. Most biological motors utilize some form of chemical energy derived from their surroundings to induce conformational changes in order to carry out specific functions. These small molecular motors operate in the presence of strong thermal fluctuations and in the regime of low Reynolds numbers, where viscous forces dominate inertial forces. Thus, their dynamical behavior is fundamentally different from that of macroscopic motors, and different mechanisms are responsible for the production of useful mechanical motion.

There is no reason why our interest should be confined to the small motors that occur naturally in biological systems. Recently, micron and nanoscale motors that use chemical energy to produce directed motion by a number of different mechanisms have been made in the laboratory. These small synthetic motors also experience strong thermal fluctuations and operate in regimes where viscous forces dominate. Potentially, these motors could be directed to perform different transport tasks, analogous to those of biological motors, for both *in vivo* and *in vitro* applications. Although some synthetic motors execute conformational changes to effect motion, the ma-



jority do not, and, instead, they use other mechanisms to convert chemical energy into directed motion.

In this Account, we describe how synthetic motors that operate by self-diffusiophoresis make use of a self-generated concentration gradient to drive motor motion. A description of propulsion by self-diffusiophoresis is presented for Janus particle motors comprising catalytic and noncatalytic faces. The properties of the dynamics of chemically powered motors are illustrated by presenting the results of particle-based simulations of sphere-dimer motors constructed from linked catalytic and noncatalytic spheres. The geometries of both Janus and sphere-dimer motors with asymmetric catalytic activity support the formation of concentration gradients around the motors. Because directed motion can occur only when the system is not in equilibrium, the nature of the environment and the role it plays in motor dynamics are described. Rotational Brownian motion also acts to limit directed motion, and it has especially strong effects for very

*To whom correspondence should be addressed

small motors. We address the following question: how small can motors be and still exhibit effects due to propulsion, even if only to enhance diffusion? Synthetic motors have the potential to transform the manner in which chemical dynamical processes are carried out for a wide range of applications.

1 Introduction

A large effort has been made in recent years to synthesize and study micron and nanoscale motors and machines. These small devices are constructed from a wide range of materials, such as DNA, polymers, or metals, take many different shapes and sizes, and, owing to such variety, are able to move using different mechanisms. They have been shown to act, at least in proof-of-concept, as walkers, shuttles, rotors, pumps, cargo carriers, muscles, and artificial flagella and cilia.¹⁻³ Some synthetic motors are designed to move as a result of nonreciprocal cyclic conformational changes, mimicking many of the motors and microorganisms found in nature. Motors that do not rely on conformational changes for motion have also been constructed, and these motors are the principal focus of this Account.

Apart from nanomotors without moving parts that are propelled by external stimuli, many such motors rely on chemical reactions for propulsion.⁴ The fuel they use is not carried by the motor itself, but, rather, it is derived from the local environment: they are active devices that use the chemical energy available in their immediate vicinity to perform work. In place of asymmetrical conformation changes, these chemically powered motors are constructed with a structural asymmetry in chemical activity that leads to directed motion. The motor motion depends on the characteristics of both the motor and its environment and their interaction with one another.

The first chemically propelled nanomotors were bimetallic rods constructed with gold and platinum or nickel portions, which, when placed in solutions containing hydrogen peroxide, were able to execute autonomous linear and rotational motions.^{5,6} Subsequently, other types of chemically driven motors were synthesized.^{3,7} Similar to bimetal-

lic rods, these motors contain two main domains that are composed of different materials, allowing for chemical reactions to occur asymmetrically on the motor. Janus particles are spherical colloids generally made from one material, half covered by another material, giving the appearance of two faces.⁸ Sphere-dimer motors are similar to Janus particles, but they comprise two linked spheres made of different materials.^{9,10} Microtubular motors are hollow cylindrical or conical tubes that have a reactive interior and inert exterior.¹¹⁻¹³ Although many of these motors rely on the same platinum-peroxide catalytic reaction, motors constructed more recently have incorporated different metals, alloys, or compounds in order to provide better control over motion or to exploit different fuels.³

Regardless of the specific motor geometry or fuel, two classes of mechanisms are largely responsible for the self-propulsion of chemically driven nanomotors.^{3,4} Bubble propulsion is due to the catalytic production of gas at the motor and the resulting recoil of the gas bubbles from the motor surface. This mechanism is usually invoked whenever bubbles are directly observed, as is the case with tubular motors, where gas accumulates in the motor interior and is expelled from one of the ends. In phoretic mechanisms, the motor self-generates some type of gradient (electrical, concentration, temperature) in its vicinity through a chemical reaction, and motion is induced by this gradient. For bimetallic rod motors, a flow of electrons in the rod between the anodic and cathodic sites of a redox reaction creates a self-generated electric field that drives ion motion in the electrical double layer surrounding the motor.¹⁴ In some situations, more than one phoretic mechanism may operate for the same motor. For example, the mechanism by which sphere dimers move is highly dependent on the rate of catalysis and surface roughness and may move either by bubble propulsion or self-diffusiophoresis.¹⁵ Both self-electrophoretic and self-diffusiophoretic mechanisms have been shown to contribute to the propulsion of the same motor.^{16,17} Simulations of Janus particles fueled by exothermic reactions have also shown that self-diffusiophoresis and self-thermophoresis may act at the same time and possibly in opposite directions.¹⁸

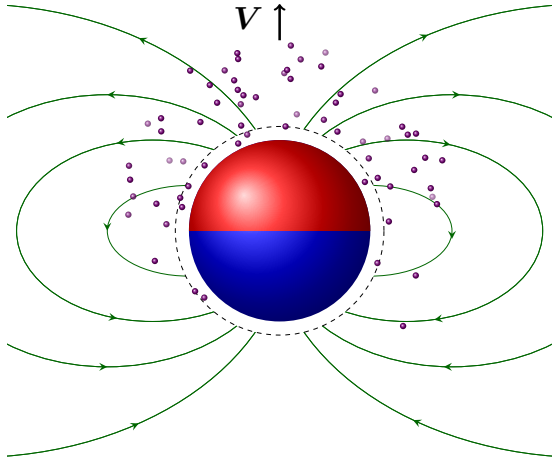


Figure 1: A Janus particle, in the laboratory frame of reference, which is self-propelled by a diffusiophoretic mechanism. The catalytic part (red, upper hemisphere) catalyzes the conversion of the fuel A molecules (not shown) to the product B molecules (small purple spheres). The chemically inactive face is the lower (blue) hemisphere. The system parameters are chosen so that \mathbf{V} points from the N to the C face. The dipolar fluid velocity field in the particle vicinity is also shown (green lines).

2 Chemically Powered Motors

The means by which small motors use chemical reactions to execute directed motion may be illustrated by considering a spherical Janus particle with catalytic (C) and noncatalytic (N) faces, which is shown in Figure 1. The dynamics of the Janus particle depends on the specific chemical reactions that are responsible for self-propulsion. Here, we suppose that a simple idealized $A \rightarrow B$ reaction takes place on the C face of the Janus particle. This model will still account for many of the generic features of real motor motion. The fluid surrounding the particle contains solvent S, fuel A, and product B chemical species.

The molecular origin of propulsion can be traced to the different interactions that the fuel and product molecules have with the Janus particle. The intermolecular potentials are assumed to be short-ranged and take non-zero values only within a thin interfacial region surrounding the Janus particle (dashed line in Figure 1). Because the catalytic activity is confined to one face of the particle, a nonuniform distribution of fuel and product molecules is produced in its vicinity. The re-

sulting concentration gradient gives rise to a force on the Janus particle. Because there are no external forces acting on the system and the intermolecular forces have short range, the Janus particle plus the solvent within the boundary layer is force-free. Through momentum conservation, a flow is generated in the surrounding fluid, and the particle is propelled in a direction opposite to the fluid flow. From these qualitative considerations, detailed theoretical expressions for the motor velocity, based on a continuum description of the motor environment, have been given previously in the literature.^{19–25} Below, we present an outline of such theoretical results, specialized to the simple $A \rightarrow B$ reaction model.

The fluid flow in the boundary region leads to a slip velocity, \mathbf{v}_s , on its outer edge at $r = R_0$, whose value depends on the concentration gradient, intermolecular forces, and solvent viscosity through the relation^{26,27}

$$\mathbf{v}_s(R_0, \theta) = \frac{k_B T}{\eta} (\Lambda_N + (\Lambda_C - \Lambda_N)H(\theta)) \nabla_\theta c_A(R_0) \quad (1)$$

where θ is the polar angle in a spherical polar coordinate system, k_B is the Boltzmann constant, η is the shear viscosity, T is the absolute temperature, c_A is the concentration of the A molecules, and the function $H(\theta)$ is defined to be unity on the catalytic C hemisphere ($0 \leq \theta \leq \pi/2$) and zero on the noncatalytic N hemisphere ($\pi/2 < \theta \leq \pi$).²⁰ In this equation, the intermolecular potentials enter through Λ_I

$$\Lambda_I = \int_0^\infty dr r \left(e^{-\beta U_{BI}(r)} - e^{-\beta U_{AI}(r)} \right) \quad (2)$$

where $\beta = 1/(k_B T)$ and $U_{\alpha I}$ is the potential of mean force between the chemical species α ($\alpha = A, B$) and the I ($I = C, N$) hemisphere of the Janus particle. The velocity of the Janus particle is given in terms of the surface (\mathcal{S}) average of the slip velocity as $\mathbf{V} = -\langle \mathbf{v}_s \rangle_{\mathcal{S}}$, where $\langle \mathbf{v}_s \rangle_{\mathcal{S}} = \int_{\mathcal{S}} \mathbf{v}_s d\mathcal{S} / (4\pi R_0^2)$. The Λ_I parameters can take either sign, and this determines the direction of propagation.

The concentration field of the A molecules is found by solving the steady-state diffusion equation, $\nabla^2 c_A = 0$, subject to a reflecting boundary condition on the noncatalytic portion of the sur-

face at R ($\approx R_0$) and a radiation boundary condition on the catalytic surface: $(D\hat{\mathbf{r}} \cdot \nabla c_A)_{r=R} = \bar{k}_0 c_A(R)H(\theta)$, where D is the relative diffusion constant of A and the Janus particle, $\hat{\mathbf{r}}$ is the unit vector along \mathbf{r} , $\bar{k}_0 = k_0/(4\pi R^2)$, and k_0 is the intrinsic reaction rate constant. Far from the particle, we assume there exists only fuel with concentration c_0 , so $c_A(r \rightarrow \infty) = c_0$. The Janus particle velocity is found by substituting the concentration field obtained from the solution of the diffusion equation into the slip-velocity equation and then taking the surface average as indicated above. The result for $V_z = \hat{\mathbf{z}} \cdot \mathbf{V}$, the motor velocity along the unit vector, $\hat{\mathbf{z}}$, from the center of the Janus particle to the pole of the C hemisphere is

$$V_z = \frac{k_B T c_0 \bar{k}_0}{\eta D} (a_C \Lambda_C + a_N \Lambda_N), \quad (3)$$

where a_I ($I = C, N$) are coefficients determined from the solution of the reaction-diffusion equation and depend on the ratio k_0/k_D , with $k_D = 4\pi R D$ the Smoluchowski rate coefficient.

This expression can be used to determine how V_z varies with system parameters. For instance, consider changing the radius R of the Janus particle. The Λ_I terms depend on the boundary layer thickness δ and particle size and vary linearly with R for $R \gg \delta$. Also, $k_0 \sim R^2$, \bar{k}_0 is independent of R , and $k_D \sim R$. The full rate coefficient for the $A \rightarrow B$ reaction may be written as $k = k_0 k_D / (k_0 + k_D)$. Then, for small Janus particles, $k_0/k_D \ll 1$, $k \approx k_0$, and we have reaction controlled kinetics. In this limit, one may show that the a_I coefficients are independent of k_0/k_D and thus the R dependence of V_z is controlled by the Λ_I terms. If, instead, the particle is large, then $k_0/k_D \gg 1$, $k \approx k_D$, and we have diffusion-controlled kinetics. The a_I coefficients now depend on R , and the nature of the R dependence requires the specific form of the solution of the reaction-diffusion equation. The precise value of R where the kinetics changes from reaction to diffusion control depends on the intrinsic reaction rate and species diffusion coefficients. These comments, along with earlier work on the size dependence of Janus particle velocity,²⁸ indicate that the motor velocity may vary in nontrivial ways as the system parameters are changed.

The fluid flow outside the interfacial layer can

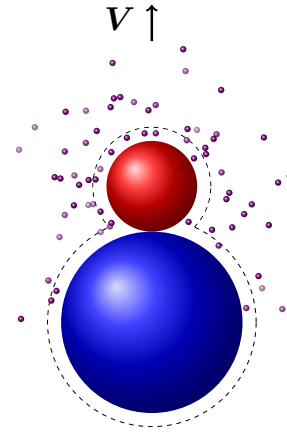


Figure 2: A sphere-dimer motor propelled by self-diffusiophoresis: the catalytic sphere (red) converts fuel molecules (not shown) to product molecules (small purple spheres). The noncatalytic sphere is depicted in blue, and the interfacial region is shown as a dashed line. The system parameters are again chosen so that \mathbf{V} points from the N to the C sphere.

be calculated from the solution to the Stokes equation, and in the laboratory frame of reference, it is given by $\mathbf{v}(\mathbf{r}) = \frac{1}{2}(R/r)^3(3\hat{\mathbf{r}}\hat{\mathbf{r}} - \mathbf{I}) \cdot \mathbf{V}$.^{26,27} The fluid-flow lines around the self-propelled Janus particle are shown in Figure 1. The dipolar form of these flow lines implies a $1/r^3$ decay of the velocity field far from the particle.

Another simple motor geometry consists of two linked catalytic and noncatalytic spheres (see Figure 2). An analysis similar to that described above for Janus particles, but technically more involved, can be carried out for these motors to obtain the velocity.²⁹

Similar analyses can be carried out for propulsion by other self-phoretic mechanisms, although some details of the calculation differ. It is important to recognize that our Janus particle example was idealized and, in applications to motor motion in the laboratory, details of the reaction mechanism and other factors may need to be taken into account.^{23,28} Bimetallic rod and Janus particle motors operate by self-electrophoresis, and the precise nature of the oxidation and reduction reactions that take place on the motor will influence its dynamics.¹⁴

3 Nanomotor Dynamics

Small chemically propelled motors are strongly influenced by thermal fluctuations. Also, as the motor size decreases to nanometer scales, the validity of macroscopic models for the dynamics should be examined to determine their applicability. For these reasons, it is appropriate to consider particle-based descriptions where the dynamics of the entire system is described by either molecular dynamics or mesoscopic dynamical schemes that retain the important features of full molecular dynamics. It is especially important to preserve momentum conservation for the reasons described earlier. The results that follow were derived from simulations using hybrid molecular dynamics (MD)-multiparticle collision dynamics (MPCD)^{30–33} or full MD, depending on the size of the motor being studied. The full MD simulations were carried out for a simple model system but could be extended to treat specific real systems. By contrast, the larger-scale MD-MPC simulations utilize coarse-grained descriptions of all species and additionally neglect solvent structural effects. Nevertheless, these simulation models account for the principal elements of self-diffusiophoretic motion.

Self-propulsion can occur only under nonequilibrium conditions since detailed balance prohibits directed motion in an equilibrium system. For sustained motion to occur, the system must be maintained in a nonequilibrium state by fluxes of reagents at the boundaries or by bulk reactions that are themselves forced out of equilibrium.

The examples of chemically powered motor dynamics given below will be confined to sphere-dimer motors since most of our simulations have been performed with this motor geometry;³⁴ however, many of the phenomena we describe are observed for other motor geometries. The investigation of the dynamics of synthetic self-propelled nanomotors is an active area of research, and there is a large amount of literature describing work in this area.^{2,3} A survey of this literature is beyond the scope of this Account. Instead, we shall highlight just a few aspects of motor dynamics that are dictated by our current interests: motor motion in complex media, collective motor motion, and the dynamics of very small molecular-scale motors.

In the biological realm, molecular motors operate in complex nonequilibrium environments where the surrounding medium supports networks of chemical reactions that supply fuel and remove product. Synthetic, chemically-powered motors may also operate in such complex chemical media, and we present two examples to illustrate the new phenomena that arise in such situations.

Consider a sphere-dimer motor where the reaction $A \rightarrow B$ on the catalytic sphere generates the chemical gradient responsible for propulsion. The medium in which the motor moves supports the nonequilibrium cubic autocatalytic reaction, $B + 2A \rightarrow 3A$, where A is the autocatalyst.³⁵ Notice that the bulk reaction consumes the product and regenerates the fuel so that motor motion may be sustained. This bulk reaction also supports the formation of a traveling chemical wave: if half of the system is initially filled with A species and the other half with B , then the autocatalyst will consume the B particles at the interface between these two regions, leading to the formation of a propagating front. A sphere-dimer motor placed in the fuel-rich A domain and oriented toward the interface will encounter the front provided its speed is greater than that of the front. Because the system is rich in product B beyond the front, the motor cannot penetrate deeply into this fuel-poor region. If the motor were oriented perpendicular to the front and orientational Brownian motion were suppressed, then the motor would propagate with the front; however, Brownian reorientation and self-propulsion will cause the motor to re-enter the fuel-rich A domain, giving rise to reflection-like dynamics in the front vicinity (see Figure 3). This feature suggests the possible control of motor motion by chemical patterns.

The medium in which the motor moves can support even more complex nonequilibrium oscillatory states. Oscillatory dynamics is commonly observed in biological systems where coupled autocatalytic reactions give rise to the periodic behavior. To study motor dynamics in such media, we again suppose that the reaction on the catalytic sphere of the sphere-dimer motor is $A \rightarrow B$. These species are also involved in bulk nonequilibrium reactions whose kinetics is controlled by the Selkov model: $S \rightleftharpoons A$, $A + 2B \rightleftharpoons 3B$, $B \rightleftharpoons S$, where S is considered to be an inert feed

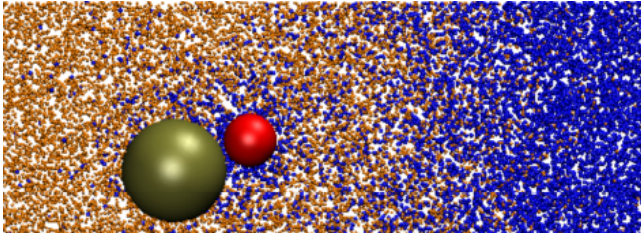


Figure 3: Propagating chemical wave and sphere dimer at one time instant.³⁵ Species A and B are rendered in red and blue, respectively. The chemical front and the self-generated concentration field around the motor can be seen in this figure.

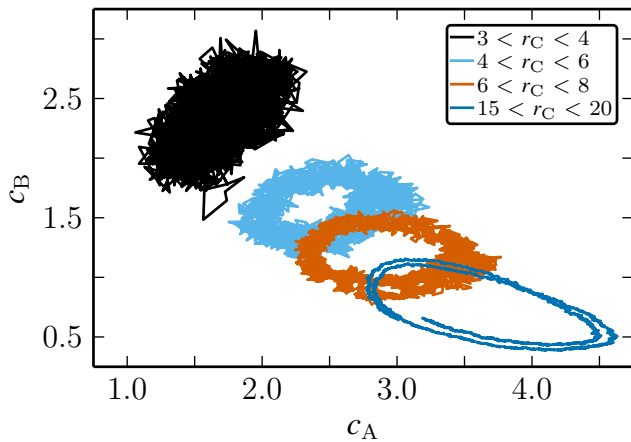


Figure 4: Concentrations of A and B are plotted over the course of several cycles. The different concentration plots correspond to the concentration in spherical shells around the catalytic sphere at different radii, r_C .

for A and B. The rate constants in these reactions can be chosen to yield an oscillatory state. The Selkov model has its antecedents as a simple model for glycolytic oscillations. Since the reaction on the dimer motor involves the same chemical species, it locally perturbs the Selkov oscillatory dynamics. In particular, the concentration of the product B species is observed to oscillate around a higher average value close to the catalytic sphere, whereas the opposite trend is seen for the fuel A concentration (see Figure 4). These shifts in the concentration cycles also create oscillations in the concentration gradient across the noncatalytic sphere, which lead to oscillations in the sphere dimer's velocity. Thus, the motor is able to influence the local chemical kinetics of an oscillatory medium and, in turn, these changes modify the motor motion.

Next, we briefly consider the collective motion of chemically powered motors. Systems containing many motors constitute active media, which have been shown to exhibit phenomena that are quite distinct from those seen in systems with inactive components. Active systems exist in out-of-equilibrium states, and the investigation of the properties of this new class of systems is a rapidly growing research area.³⁶ The active constituents can have diverse length scales, ranging from the large macroscopic sizes of birds in flocks or fish in schools, to micron-sized swimming organisms. In these examples, the active objects are powered internally but are sustained by the input of food sources. Models for such systems often assign a velocity to individual active objects and interactions of various kinds among the objects lead to nontrivial collective behavior.

The collective motion of chemically powered motors has been studied experimentally^{37,38} and theoretically.^{39–41} Phenomena, such as active self-assembly into dynamical clusters with various geometries and swarming behavior, have been observed. Several factors have to be taken into account when the dynamics of an ensemble of chemically powered motors is considered. Each self-propelled motor generates its own concentration gradient. This gives rise to a chemotactic response that typically causes motors to be attracted to each other, analogous in some respects to the chemotactic response of bacteria to high food concentrations.⁴² The chemotactic response of synthetic nanomotors to chemical gradients has been observed in experiments.^{43,44} Also, each motor induces a flow field in the surroundings, and one motor can perturb the flow field of its neighbors, leading to a hydrodynamic coupling among motors. The motors may also interact directly through short- or long-range interactions, and because of all of these interactions, the collective dynamics may be complicated.

Earlier studies of the collective behavior of chemically powered motors considered ensembles of identical motors.^{39–41} An even richer phenomenology is found when the ensemble consists of motors of two types that can couple through chemical reactions. Consider an ensemble of types I and II sphere-dimer motors, which interact through chemical gradients in the following

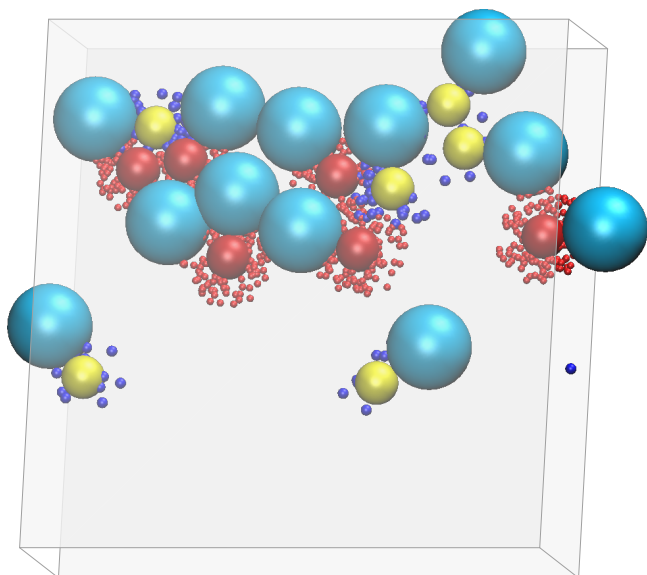


Figure 5: An instantaneous configuration showing the collective behavior of a mixture of types I (red catalytic sphere) and II (yellow catalytic sphere) sphere-dimer nanomotors. The product species B (red) and C (blue) are shown only in the immediate vicinities of the motors.

way: the product of a type I motor is the fuel for a type II motor. In particular, type I motors catalyze the reaction $A \rightarrow B$, whereas type II motors catalyze the reaction $B \rightarrow C$. This is an example of a system where the motors themselves participate in networks of chemical reactions. If the system is supplied with fuel A, then motors of type II will not actively move unless they are in the vicinity of motors of type I, which provide their fuel. An instantaneous configuration that is formed in the course of the evolution is shown in Figure 5. The type I motors actively aggregate into dynamical clusters, and the type II motors tend to aggregate on the surfaces of these clusters. Both theoretical and experimental investigations of the collective behavior of chemically powered motors are at an early stage, and significant progress is anticipated in this area.

4 Fluctuations and Diffusion

While the chemical concentration gradient generated by the motor determines its propagation direction and affects its speed, orientational Brownian motion will change the direction in which it moves

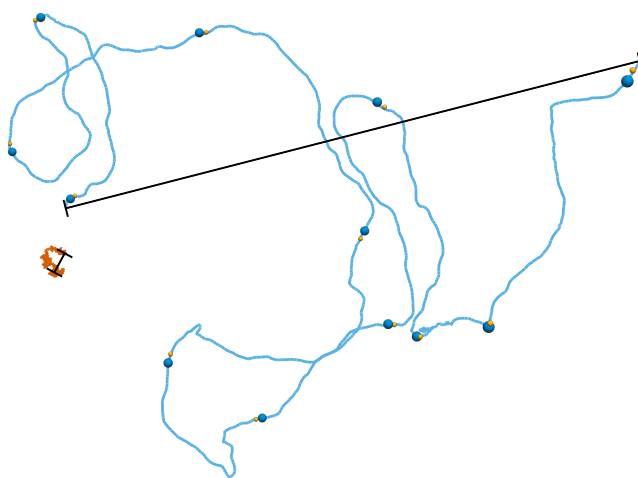


Figure 6: Trajectory of a nanoscale sphere-dimer motor (sky blue). For comparison, a trajectory of the same duration is shown for an inactive dimer (no motor reactions) is also shown (vermilion). The reactive dimer travels a 40 times greater end-to-end distance (black) than the inactive dimer.

so that on sufficiently long time scales the directed motion will manifest itself as enhanced diffusion. The enhanced diffusion is evident from a comparison of the two trajectories in Figure 6, corresponding to chemically active and inactive dimers. Only for times less than the orientational time will the ballistic motion of the motor be evident. A number of important questions arise when the effects of fluctuations on motor dynamics are considered. How far, on average, does the motor move before the ballistic motion is masked by Brownian motion? How is the diffusion coefficient modified by directed motion? What is the lower limit on the size of the motor for self-diffusiophoresis to operate? For micron and large nanoscale motors, the answers to these questions will determine how effectively the motor can carry out transport tasks and what control scenarios must be implemented to overcome the effects of rotational Brownian motion. If such motors are ever to be used on scales comparable to the interior of a cell, it is important to determine if they can be made to operate when they are only a few nanometers in size.

The mean square displacement (MSD), $\Delta L^2(t)$, of the center of mass of the motor provides some information that can be used to answer these questions. We may write the motor velocity as the sum of the average velocity along the instanta-

neous bond unit vector $\hat{\mathbf{z}}(t)$, and a fluctuation $\delta\mathbf{V}(t)$, $\mathbf{V}(t) = \langle V_z \rangle \hat{\mathbf{z}}(t) + \delta\mathbf{V}(t)$. Assuming exponential decay for the orientational $\langle \hat{\mathbf{z}}(t) \cdot \hat{\mathbf{z}} \rangle = e^{-t/\tau_r}$ and velocity fluctuation $\langle \delta\mathbf{V}(t) \cdot \delta\mathbf{V} \rangle = (3k_B T/M_m) e^{-t/\tau_v}$ correlation functions, the MSD takes the form

$$\Delta L^2(t) = 6D_m t - 2\langle V_z \rangle^2 \tau_r^2 \left(1 - e^{-t/\tau_r}\right) - 6\frac{k_B T}{M_m} \tau_v^2 \left(1 - e^{-t/\tau_v}\right) \quad (4)$$

Here, τ_r and τ_v are the reorientation and velocity relaxation times, and M_m is the motor mass. The effective dimer diffusion coefficient is $D_m = D_0 + \frac{1}{3}\langle V_z \rangle^2 \tau_r$, where $D_0 = (k_B T/M_m) \tau_v$. In the ballistic regime, $t \ll \tau_v$, $\Delta L^2(t) \approx (3k_B T/M_m + \langle V_z \rangle^2) t^2$.

The majority of research has been carried out on chemically self-propelled motors with linear dimensions of microns or hundreds of nanometers, similar to those of many swimming microorganisms. Typical motor velocities are in the range of tens of micrometers per second but could be even higher. Given the motor speeds and sizes, and the kinematic viscosity of water, this places these motors in the low Reynolds number regime.

If one scales down by 2 to 3 orders of magnitude to the regime where motor linear dimensions are a few nanometers, the effects of fluctuations are a dominant factor, and it is interesting to investigate the dynamical properties of these tiny motors. They now have sizes comparable to those of many protein motors and machines in the cell. Experimental observations of artificial self-propelled motors at the molecular scale, Janus particles of 30 nm size⁴⁵ down to organometallic motors of 5 Å size,⁴⁶ show enhanced diffusion even at this small length scale.

Ångström-size chemically powered motors⁴⁷ have been studied theoretically using molecular dynamics. These tiny motors employ the same mechanism of propulsion through diffusiophoresis as that of larger nanoscale and micron-size motors; in this regime, however, whose motion is subject to very strong fluctuations and solvent structural effects given the comparable sizes of motor and solvent molecules. The mean-square displacements of an Ångström-size sphere dimer and a nanoscale sphere dimer are shown in Figure 7, where time

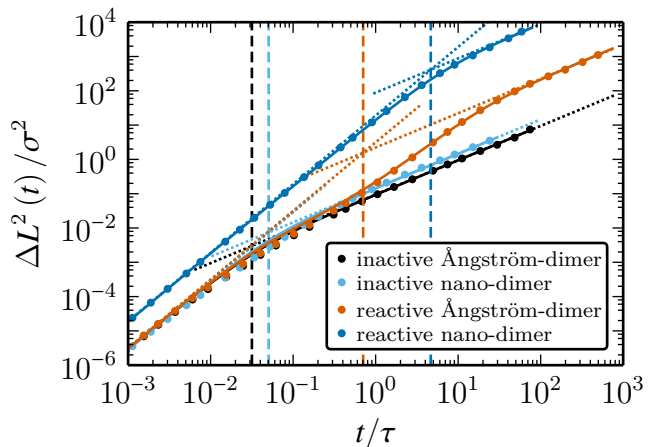


Figure 7: Mean-square displacements of inactive and reactive Ångström-scale and nanoscale sphere dimers. The points show simulation data, and the solid lines show theoretical predictions. The vertical dashed lines indicate crossover times between the short-time ballistic and the long-time diffusive regimes. The data is shown in dimensionless time and length units of $\tau = \sigma \sqrt{M_m/k_B T}$ and $\sigma = \sqrt[3]{d_C^3 + d_N^3}$, respectively, where d_C and d_N are the diameters of the C and N spheres.

and length have been rescaled to account for their different sizes and thermal velocity. For both length scales, the simulation data is in good agreement with the theoretical prediction in eq (4). The rescaled MSDs of the inactive dimers, their motion is subject only to thermal fluctuations, is approximately equal and thus independent of the length scale. The rescaled MSD of the reactive dimers, however, reveals significant differences depending on the length scale. In the ballistic regime, $t \ll \tau_v$, the MSD of the reactive nanodimer is significantly larger than that of the inactive nanodimer, since the thermal velocity $(k_B T/M_m)^{1/2}$ is negligible compared to the average propulsion velocity $\langle V_z \rangle$, and $\Delta L^2(t) \approx \langle V_z \rangle^2 t^2$. The MSD of the reactive Ångström-dimer, however, is almost equal to that of the inactive Ångström-dimer, since now the propulsion velocity is negligible compared to the thermal velocity, and $\Delta L^2(t) \approx (3k_B T/M_m) t^2$. In the diffusive regime, $t \gg \tau_r$, both the reactive Ångström-dimer and the reactive nanodimer exhibit enhanced diffusion, where the enhancement is smaller (but still significant) for the Ångström-dimer, as expected due to the stronger thermal fluctuations. The crossover regime from the ballistic

to the diffusive regime is short for the nanodimer; for the Ångström-dimer, however, the crossover regime spans 3 orders of magnitude in (rescaled) time. Given $\langle V_z \rangle$ and τ_r , the average linear distance traveled by a motor can be estimated as $\langle V_z \rangle \tau_r$. The reactive nanodimer travels an average distance of 11.6 times its effective diameter, σ ; the Ångström-dimer travels 3.0 times its effective diameter. Thus, chemically powered motors can operate on very small length scales and yield substantially enhanced diffusion coefficients, consistent with recent experiments on active enzymes^{48,49} and small Janus-like particles.⁴⁵ These observations suggest possible applications using very small synthetic motors.

5 Conclusions

Investigations of small chemically powered motors present challenges for experiment and theory. They may also provide a diverse and transformative range of tools for new applications. Experimental challenges center around the design and construction of micron and nanoscale motors with specific geometries, fueled by various chemicals, operating by propulsion and control mechanisms selected for specific purposes. Since motors that might be used for some tasks may be very small, continuum descriptions, while often applicable on surprisingly small length and time scales, may nevertheless break down, and this necessitates the use of microscopic or mesoscopic theories of the dynamics. Self-propelled motors function under nonequilibrium conditions, and their full statistical mechanical description must account for the fluxes that drive the system out of equilibrium. In far-from-equilibrium regimes, systems display features, such as bistability, oscillations, and self-propulsion, that are distinct from those of equilibrium systems. The statistical mechanics of driven nonequilibrium systems is a topic of current research, and complete studies of chemically powered motors within this context have not yet been carried out.

The potential uses of nanomotors have been discussed often in articles and reviews, and proof-of-principle experiments have shown that operations, such as cargo transport and motor-aided microflu-

idic flows, may soon lead to viable applications. Other applications, particularly those that involve biological systems, will require the development of motors that use biocompatible fuels and motor components. In most cases, a single nanomotor is insufficient to complete a task. A full understanding of the factors that lead to the collective behavior of motors, the spatiotemporal structures that develop, and methods needed to control ensembles of interacting motors must be achieved before many applications can be carried out. When such issues concerning motor design and control are completely understood, it is possible that synthetic motors and active transport will play as significant a role as molecular motors and machines currently play in living systems.

Author Information

Biographies

Peter H. Colberg received his Diplom in physics from the Ludwig-Maximilians-Universität München. He is currently a Ph.D. candidate at the University of Toronto, where he studies chemically powered motors using microscopic and mesoscopic models. He composes large-scale molecular simulation programs for highly parallel processors such as GPUs.

Shang Yik Reigh received his Ph.D. from Seoul National University. He has postdoctoral research experience from the Forschungszentrum Jülich and the University of Toronto. His research interests are in the theory and simulation of diffusion-controlled reactions, polymer melts, bacterial locomotion, and self-propelled nanomotors.

Bryan Robertson received his B.Sc. in Chemistry from the University of Western Ontario in 2013. He is currently a Ph.D. student at the University of Toronto, studying the behavior of nanomotors in complex media.

Raymond Kapral received his Ph.D. from Princeton University and pursued postdoctoral studies at the Massachusetts Institute of Technology. He is currently Professor of Chemistry at the University of Toronto. His research interests lie in

the areas of nonequilibrium statistical mechanics and quantum dynamics.

Acknowledgments

This work was supported in part by a grant from the Natural Sciences and Engineering Research Council of Canada and Compute Canada.

References

- 1 Kay, E. R.; Leigh, D. A.; Zerbetto, F. Synthetic molecular motors and mechanical machines. *Angew. Chem., Int. Ed.* **2007**, *46*, 72–191.
- 2 Jones, R. A. L. *Soft Machines: Nanotechnology and Life*; Oxford University Press: Oxford, UK, 2004.
- 3 Wang, J. *Nanomachines: Fundamentals and Applications*; Wiley-VCH: Weinheim, Germany, 2013.
- 4 Kapral, R. Perspective: Nanomotors without moving parts that propel themselves in solution. *J. Chem. Phys.* **2013**, *138*, 020901.
- 5 Paxton, W. F.; Kistler, K. C.; Olmeda, C. C.; Sen, A.; Angelo, S. K. S.; Cao, Y.; Mallouk, T. E.; Lammert, P. E.; Crespi, V. H. Catalytic nanomotors: autonomous movement of striped nanorods. *J. Am. Chem. Soc.* **2004**, *126*, 13424–13431.
- 6 Fournier-Bidoz, S.; Arsenault, A. C.; Manners, I.; Ozin, G. A. Synthetic self-propelled nanomotors. *Chem. Commun.* **2005**, 441–443.
- 7 Wang, W.; Duan, W.; Ahmed, S.; Mallouk, T. E.; Sen, A. Small power: autonomous nano- and micromotors propelled by self-generated gradients. *Nano Today* **2013**, *8*, 531–554.
- 8 Howse, J. R.; Jones, R. A. L.; Ryan, A. J.; Gough, T.; Vafabakhsh, R.; Golestanian, R. Self-motile colloidal particles: from directed propulsion to random walk. *Phys. Rev. Lett.* **2007**, *99*, 048102.
- 9 Rückner, G.; Kapral, R. Chemically powered nanodimers. *Phys. Rev. Lett.* **2007**, *98*, 150603.
- 10 Valadares, L. F.; Tao, Y.-G.; Zacharia, N. S.; Kitaev, V.; Galembeck, F.; Kapral, R.; Ozin, G. A. Catalytic nanomotors: self-propelled sphere dimers. *Small* **2010**, *6*, 565–572.
- 11 Mei, Y.; Huang, G.; Solovev, A.; Ureña, E. B.; Mönch, I.; Ding, F.; Reindl, T.; Fu, R.; Chu, P.; Schmidt, O. Versatile approach for integrative and functionalized tubes by strain engineering of nanomembranes on polymers. *Adv. Mater.* **2008**, *20*, 4085–4090.
- 12 Soler, L.; Magdanz, V.; Fomin, V. M.; Sanchez, S.; Schmidt, O. G. Self-propelled micromotors for cleaning polluted water. *ACS Nano* **2013**, *7*, 9611–9620.
- 13 Zhao, G.; Ambrosi, A.; Pumera, M. Clean room-free rapid fabrication of roll-up self-powered catalytic microengines. *J. Mater. Chem. A* **2014**, *2*, 1219–1223.
- 14 Wang, Y.; Hernandez, R. M.; Bartlett, D. J., Jr.; Bingham, J. M.; Kline, T. R.; Sen, A.; Mallouk, T. E. Bipolar electrochemical mechanism for the propulsion of catalytic nanomotors in hydrogen peroxide solutions. *Langmuir* **2006**, *22*, 10451–10456.
- 15 Wang, S.; Wu, N. Selecting the swimming mechanisms of colloidal particles: bubble propulsion versus self-diffusiophoresis. *Langmuir* **2014**, *30*, 3477–3486.
- 16 Ebbens, S.; Gregory, D. A.; Dunderdale, G.; Howse, J. R.; Ibrahim, Y.; Liverpool, T. B.; Golestanian, R. Electrokinetic effects in catalytic platinum-insulator Janus swimmers. *EPL* **2014**, *106*, 58003.
- 17 Brown, A.; Poon, W. Ionic effects in self-propelled Pt-coated Janus swimmers. *Soft Matter* **2014**, *10*, 4016–4027.
- 18 de Buyl, P.; Kapral, R. Phoretic self-propulsion: a mesoscopic description of reaction dynamics that powers motion. *Nanoscale* **2013**, *5*, 1337–1344.

- 19 Golestanian, R.; Liverpool, T. B.; Ajdari, A. Propulsion of a molecular machine by asymmetric distribution of reaction products. *Phys. Rev. Lett.* **2005**, *94*, 220801.
- 20 Golestanian, R.; Liverpool, T. B.; Ajdari, A. Designing phoretic micro- and nanoswimmers. *New J. Phys.* **2007**, *9*, 126.
- 21 Jülicher, F.; Prost, J. Generic theory of colloidal transport. *Eur. Phys. J.* **2009**, *29*, 27–36.
- 22 Popescu, M. N.; Dietrich, S.; Tasinkevych, M.; Ralston, J. Phoretic motion of spheroidal particles due to self-generated solute gradients. *Eur. Phys. J. E* **2010**, *31*, 351–367.
- 23 Sabass, B.; Seifert, U. Dynamics and efficiency of a self-propelled, diffusiophoretic swimmer. *J. Chem. Phys.* **2012**, *136*, 064508.
- 24 Sharifi-Mood, N.; Koplek, J.; Maldarelli, C. Diffusiophoretic self-propulsion of colloids driven by a surface reaction: The sub-micron particle regime for exponential and van der Waals interactions. *Phys. Fluids* **2013**, *25*, 012001.
- 25 Michelin, S.; Lauga, E. Phoretic self-propulsion at finite Péclet numbers. *J. Fluid Mech.* **2014**, *747*, 572.
- 26 Anderson, J. L. Transport mechanisms of biological colloids. *Ann. N.Y. Acad. Sci.* **1986**, *469*, 166–177.
- 27 Anderson, J. L. Colloid transport by interfacial forces. *Ann. Rev. Fluid Mech.* **1989**, *21*, 61–99.
- 28 Ebbens, S.; Tu, M.-H.; Howse, J. R.; Golestanian, R. Size dependence of the propulsion velocity for catalytic Janus-sphere swimmers. *Phys. Rev. E* **2012**, *85*, 020401.
- 29 Popescu, M. N.; Tasinkevych, M.; Dietrich, S. Pulling and pushing a cargo with a catalytically active carrier. *EPL* **2011**, *95*, 28004.
- 30 Malevanets, A.; Kapral, R. Mesoscopic model for solvent dynamics. *J. Chem. Phys.* **1999**, *110*, 8605–8613.
- 31 Malevanets, A.; Kapral, R. Solute molecular dynamics in a mesoscale solvent. *J. Chem. Phys.* **2000**, *112*, 7260–7269.
- 32 Kapral, R. Multiparticle collision dynamics: simulation of complex systems on mesoscales. *Adv. Chem. Phys.* **2008**, *140*, 89–146.
- 33 Gompper, G.; Ihle, T.; Kroll, D. M.; Winkler, R. G. Multi-particle collision dynamics: a particle-based mesoscale simulation approach to the hydrodynamics of complex fluids. *Adv. Polym. Sci.* **2009**, *221*, 1–87.
- 34 Tao, Y.-G.; Kapral, R. Design of chemically propelled nanodimer motors. *J. Chem. Phys.* **2008**, *128*, 164518.
- 35 Thakur, S.; Chen, J.-X.; Kapral, R. Interaction of a chemically propelled nanomotor with a chemical wave. *Angew. Chem., Int. Ed.* **2011**, *50*, 10165–10169.
- 36 Marchetti, M. C.; Joanny, J. F.; Ramaswamy, S.; Liverpool, T. B.; Prost, J.; Rao, M.; Simha, R. A. Hydrodynamics of soft active matter. *Rev. Mod. Phys.* **2013**, *85*, 1143–1189.
- 37 Theurkauff, I.; Cottin-Bizonne, C.; Palacci, J.; Ybert, C.; Bocquet, L. Dynamic clustering in active colloidal suspensions with chemical signaling. *Phys. Rev. Lett.* **2012**, *108*, 268303.
- 38 Buttinoni, I.; Bialké, J.; Kümmel, F.; Löwen, H.; Bechinger, C.; Speck, T. Dynamic clustering and phase separation in suspensions of self-propelled colloidal particles. *Phys. Rev. Lett.* **2013**, *110*, 238301.
- 39 Thakur, S.; Kapral, R. Collective dynamics of self-propelled sphere dimer motors. *Phys. Rev. E* **2012**, *85*, 026121.
- 40 Soto, R.; Golestanian, R. Self-assembly of catalytically active colloidal molecules: tailoring activity through surface chemistry. *Phys. Rev. Lett.* **2014**, *112*, 068301.
- 41 Saha, S.; Golestanian, R.; Ramaswamy, S. Clusters, asters, and collective oscillations in chemotactic colloids. *Phys. Rev. E* **2014**, *89*, 062316.

- 42 Berg, H. C. *E. coli in Motion*; Springer-Verlag: New York, 2004.
- 43 Hong, Y.; Blackman, N. M. K.; Kopp, N. D.; Sen, A.; Velegol, D. Chemotaxis of nonbiological colloidal rods. *Phys. Rev. Lett.* **2007**, *99*, 178103.
- 44 Baraban, L.; Harazim, S. M.; Sanchez, S.; Schmidt, O. G. Chemotactic behavior of catalytic motors in microfluidic channels. *Angew. Chem., Int. Ed.* **2013**, *125*, 5662–5666.
- 45 Lee, T.-C.; Alarcón-Correa, M.; Miksch, C.; Hahn, K.; Gibbs, J. G.; Fischer, P. Self-propelling nanomotors in the presence of strong brownian forces. *Nano Lett.* **2014**, *14*, 2407–2412.
- 46 Pavlick, R. A.; Dey, K. K.; Sirjoosingh, A.; Benesi, A.; Sen, A. A catalytically driven organometallic molecular motor. *Nanoscale* **2013**, *5*, 1301–1304.
- 47 Colberg, P. H.; Kapral, R. Ångström-scale chemically powered motors. *EPL* **2014**, *106*, 30004.
- 48 Muddana, H. S.; Sengupta, S.; Mallouk, T. E.; Sen, A.; Butler, P. J. Substrate catalysis enhances single-enzyme diffusion. *J. Am. Chem. Soc.* **2010**, *132*, 2110–2111.
- 49 Sengupta, S.; Dey, K. K.; Muddana, H. S.; Tabouillot, T.; Ibele, M. E.; Butler, P. J.; Sen, A. Enzyme molecules as nanomotors. *J. Am. Chem. Soc.* **2013**, *135*, 1406–1414.